

## **Analytical Modeling of Balanced and Unbalanced Short-Circuits of SMPM Motors – Analyses of Currents, Torque and PM Eddy-Current Losses**

ML. Sough<sup>1,2</sup>, D. Depernet<sup>2</sup>, F. Dubas<sup>2</sup>, B. Boualem<sup>1</sup> and C. Espanet<sup>2</sup>

<sup>1</sup>ALSTOM Transport, <sup>2</sup>FEMTO-ST

<sup>1</sup>Avenue de LATTRE de TASSIGNY, F-25290 Ornans

<sup>2</sup>ENISYS Department, UFC, FEMTO-ST Institute, UMR 6174 CNRS, F-90010 Belfort

<sup>1</sup>Ornans, <sup>2</sup>Belfort, France

Tel.: +33 / (0) – 6.59.65.05.54.

E-Mail: mohand.sough@gmail.com

URL: <http://www.femto-st.fr>

### **Keywords**

Permanent-magnet synchronous machines, short-circuit, Fortescue transformation, PM eddy-current losses, analytical model.

### **Abstract**

In this paper, the authors present an analytical modeling of short-circuit currents, corresponding electromagnetic torque and permanent-magnet (PM) eddy-current losses to resistance-limited (i.e., without eddy-current reaction field) during fault operations. Three short-circuits types are considered: on the one hand balanced three-phase short-circuit, and on the other hand unbalanced two-phase and asymmetrical short-circuits. The main results of this work are the time evolution of short-circuit currents and corresponding torque reinforced by numerical and experimental validation. Moreover, using Fortescue transformation the permanent-magnet losses are calculated during unbalanced short circuit.

### **Introduction**

Since last decade, the permanent-magnet surface-mounted (PMSM) motors are more and more often used for railway applications. And, for railway equipments manufacturers, one of the most important goals is to ensure passenger safety. In addition to that, the equipment operator must meet deadlines and ensure continuity of service.

Regarding the modeling of short-circuit proposed in this paper, the authors are mainly interested in the PM eddy-current losses estimation during unbalanced short-circuits (two-phase short-circuit). Indeed, these ones are potentially the most damaging for the electrical machine, due to the existence of both direct and inverse rotating magnetic fields. In steady state, these two fields can be calculated using Fortescue's transformation [1], so that it is finally possible to apply classical analytical model (AM) of the PM eddy-current losses, considering successively the two fields and superposing the results.

In addition, it is important to remark, that the three and two-phase short-circuits can't be solved by electrically disconnecting the machine, since those short-circuits are internal and thus are effective until the rotor rotates. This highlights the importance of modeling this phenomenon in order to predict the machine behavior and thus reduce overheating risks and farther to prevent partial or total demagnetization risk of permanent magnet especially for surface mounted PM machines [2].

An interesting analysis of symmetrical and asymmetrical short-circuit faults are presented in [3] for IPM synchronous machine and some design considerations are proposed based on [4] conclusions. In [5] an interesting observation of machine behavior in case of three-phase short-circuit are given where the others report the partial demagnetization risk of permanent magnet. In this paper, we will present the analytical modeling of short-circuit currents in the next part. Then, we present the approach to model the unbalanced behavior of the machine using Fortescue transformation. With this approach, the PM eddy-current losses and the electromagnetic torque are analytically calculated during a short-circuit and finally, experimental results are presented to validate the analytical calculation of currents and torque.

## Analytical modeling of short-circuit currents

The proposed short-circuit can be simulated by using the electrical circuit shown in the diagram of Figure 1 and by modifying the states of the switches, as follows:

- three-phase short-circuit: switches I1 to I5 are closed while others are open; the resulting simplified diagram is shown in Figure 3-(a);
- two-phase short-circuit (phase 1 and 2): the switches I1, I2 et I4 are closed while others are open; the resulting simplified diagram is shown in Figure 3-(b);

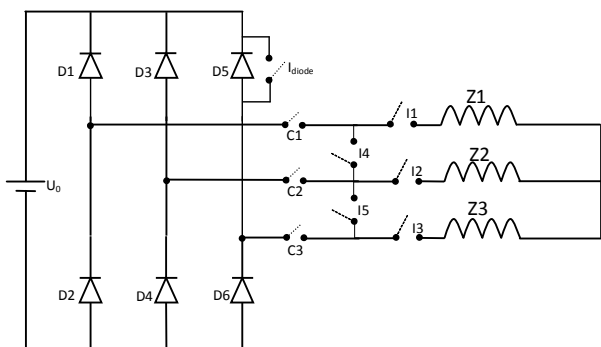


Fig.1 : Studied general short-circuit diagram

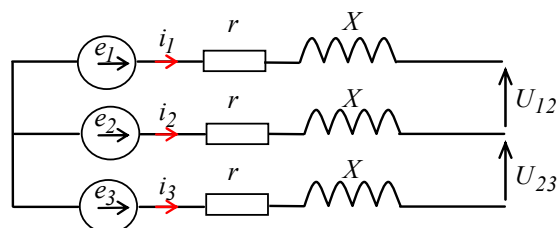
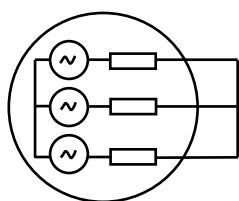
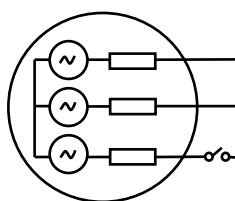


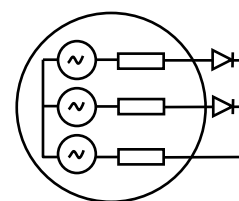
Fig.2 : Three-phase equivalent circuit



(a) Three-phase short-circuit



(b) Two-phase short-circuit



(c) Asymmetrical short-circuit

Fig.3 : Studied short-circuits

- asymmetrical short-circuit: the switches I4 et I5 are open while others are closed; the resulting simplified diagram is shown in Figure 3-(c);

The three-phase equivalent circuit of the SMPM motor is presented in Figure 2, where  $e_x$  is the back electromotive force (EMF),  $r$  and  $X = \omega \cdot L_{c,n}$  are respectively the resistance and reactance of phase.

Thus we can study the different short-circuits:

a. three-phase short-circuit: 
$$\begin{cases} U_{12} = U_{23} = 0 \\ i_1 + i_2 + i_3 = 0 \end{cases}$$

b. two-phase short-circuit (phase 1 and 2): 
$$\begin{cases} U_{12} = 0 \\ i_3 = 0 \end{cases}$$

The circuit in Figure 3 leads to the following equations:

$$\begin{cases} U_{12,n}(t) - E_{12,n}(t) = \frac{1}{\tau} \cdot i_{12,n}(t) + \frac{d}{dt} i_{12,n}(t) \\ U_{23,n}(t) - E_{23,n}(t) = \frac{1}{\tau} \cdot i_{23,n}(t) + \frac{d}{dt} i_{23,n}(t) \end{cases} \quad \text{where} \quad \begin{cases} i_{12,n}(t) = i_{1,n}(t) - i_{2,n}(t), i_{23,n}(t) = (i_{2,n}(t) - i_{3,n}(t)) \\ E_{12,n}(t) = e_{1,n}(t) - e_{2,n}(t), E_{23,n}(t) = e_{2,n}(t) - e_{3,n}(t) \end{cases} \quad (1)$$

The transformed currents,  $i_{12}$  and  $i_{23}$ , are determined by solving differential equation system (1). We thus obtain:

$$i_{12}(t) = \sum_n \left( A_{12,n} \cdot e^{-\frac{t}{\tau}} + I_{\alpha,n}(n) \cdot \sin(n\omega t - \beta_{12,n}) \right) \text{ and } i_{23}(t) = \sum_n \left( A_{23,n} \cdot e^{-\frac{t}{\tau}} + I_{\alpha,n}(n) \cdot \sin(n\omega t - \beta_{23,n}) \right) \quad (2)$$

with :

$$I_{\alpha,n}(n) = 2 \cdot \Omega_1 \cdot S_{cylc} \cdot \frac{E_m(n)}{\sqrt{r^2 + (n \cdot \omega \cdot L_{c,n})^2}} \cdot \sin\left(\frac{n \cdot \pi}{3}\right)$$

$$E_m(n) = n \cdot B_{rac} \cdot S_{cylc} \cdot \frac{p \cdot R_{sc}}{b_{oec}} \cdot K_m(n) \cdot \left[ C_I(n) + D_I(n) \cdot \left(\frac{R_a}{R_{sc}}\right)^{n-p+1} \right]$$

$$A_{12,n} = I_{\alpha,n}(n) \cdot \sin(\beta_{12,n} + \Theta_{rs0}) \text{ and } A_{23,n} = I_{\alpha,n}(n) \cdot \sin(\beta_{23,n} + \Theta_{rs0})$$

$$\beta_{12,n} = \arctan\left(\frac{\omega \cdot L_{c,n}}{r}\right) + n \cdot \frac{5 \cdot \pi}{6} \text{ and } \beta_{23,n} = \arctan\left(\frac{\omega \cdot L_{c,n}}{r}\right) + n \cdot \frac{3 \cdot \pi}{2}$$

where  $\tau = r/L_c$  is the time-constant,  $n$  the harmonic rank,  $B_{rac}$  is residual induction of PM,  $S_{cylc} = 2\pi \cdot R_{sc} \cdot L_m$  is the air gap surface,  $p$  is the number of pole pairs,  $R_{sc}$  the radius of the stator surface corrected by Carter's coefficient,  $L_m$  is active machine length,  $\Theta_{rs}(t) = \Omega_0 \cdot t + \Theta_{rs0}$  is the rotor position relative to stator as function of time,  $\Theta_{rs0}$  is the rotor initial position,  $b_{oec}$  is the slot opening corrected by Carter's coefficient,  $K_m(n)$  is the winding factor defined in [6],  $R_r$  and  $R_a$  are respectively the rotor and PM surface radius,  $\alpha_p$  is the pole pitch,  $C_I(n)$  and  $D_I(n)$  are integration constants defined as follows :

$$C_I(n) = \frac{2}{n \cdot (1 - (n \cdot p)^2)} \cdot \frac{\left[ (1 + np) \cdot \left(\frac{R_r}{R_a}\right)^{2np} + (1 - np) - 2 \cdot \left(\frac{R_r}{R_a}\right)^{np+1} \right]}{\pi \left[ 1 - \left(\frac{R_r}{R_{sc}}\right)^{2np} \right]} \cdot \left(\frac{R_a}{R_{sc}}\right)^{np+1} \sin\left(n \cdot \alpha_p \cdot \frac{\pi}{2}\right)$$

$$D_I(n) = C_I(n) \cdot \left(\frac{R_a}{R_{sc}}\right)^{-(np+1)}$$

Therefore, for each short-circuit, it is possible to determine the integration coefficients and to express the currents, as following:

*Three-phase short-circuit*

$$\begin{cases} i_1(t)_{3ph} = \frac{2}{3} \cdot i_{12}(t) + \frac{1}{3} \cdot i_{23}(t) \\ i_2(t)_{3ph} = \frac{1}{3} \cdot i_{23}(t) - \frac{1}{3} \cdot i_{12}(t) \\ i_3(t)_{3ph} = -\frac{1}{3} \cdot i_{12}(t) - \frac{2}{3} \cdot i_{23}(t) \end{cases}$$

*Two-phase short-circuit*

$$\begin{cases} i_1(t)_{2ph} = \frac{1}{2} \cdot i_{12}(t) \\ i_2(t)_{2ph} = -i_1(t)_{2ph} \\ i_3(t)_{2ph} = 0 \end{cases}$$

*Asymmetrical short-circuit*

$$\begin{cases} i_1(t)_{asy} = i_1(t)_{3ph} - |i_1(t)_{3ph}| \\ i_2(t)_{asy} = i_2(t)_{3ph} - |i_2(t)_{3ph}| \\ i_3(t)_{asy} = -[i_1(t)_{asy} + i_2(t)_{asy}] \end{cases}$$

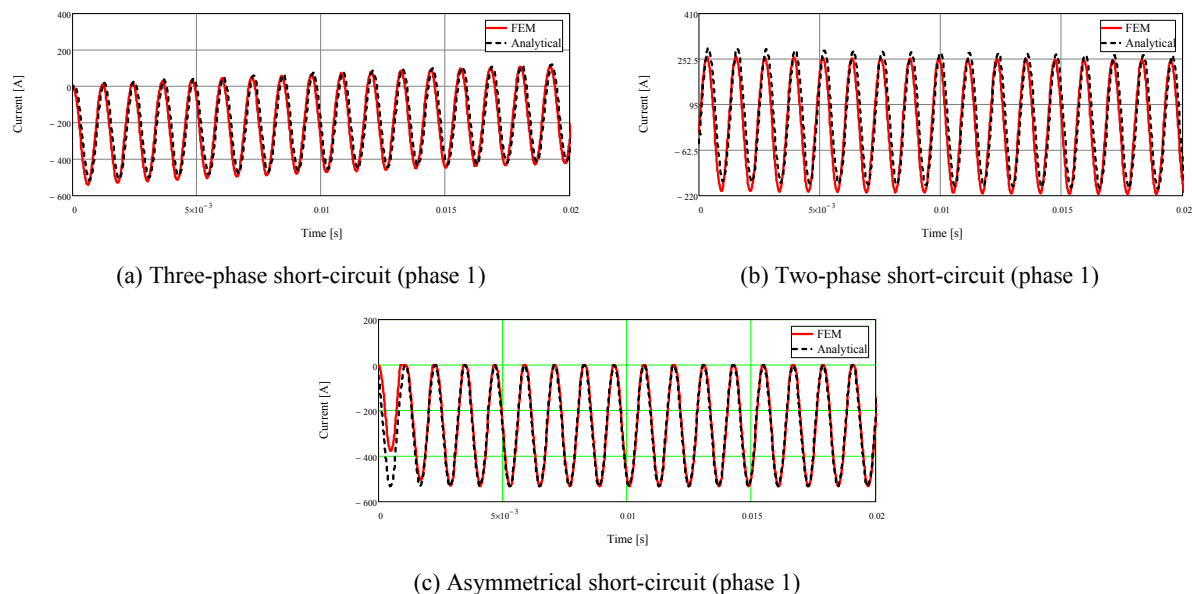


Fig.4 : Short-circuits currents comparison : FEM Vs Analytical

It can be noticed that the analytical formulations of asymmetrical short-circuits current are derived from those of three-phase short-circuit (see Figure 3-(a) and (c)). However, in the case of the unbalanced short-circuit (see Figure 3-(c)), the diodes force the currents of the first and second phase to flow in a single direction, which is opposite to that of the third phase.

To validate the proposed modeling, 2-D finite-element simulations were performed to study the various cases of short-circuit mentioned above and analyze the results.

From Figure 4, we can notice that both transient and steady state currents, during short-circuit, are accurately modeled. As it can be observed, the asymmetrical short-circuit currents being deducted from steady state three-phase short-circuit, their transient is not correctly modeled as shown in Figure 4-(c). In addition, it can be verified that the presence of diodes leads an unidirectional flow of the current. For the asymmetrical short-circuit presented here (where diode D5 is shorted), the diode D6 forces currents of Phase 1 and Phase 2 to be negative and makes that Phase 3 current is necessarily positive.

## Unbalanced systems study (two-phase short-circuit)

In order to study unbalanced systems we can use Fortescue well known transformation [1], which will be quite useful to analytically predict the generated PM eddy-current losses in steady state. This method enables the substitution of the real unbalanced system (two-phase short-circuit in our study) by two balanced systems, so-called direct and inverse systems.

Let us consider that the electrical working is purely sinusoidal, then the sinusoidal three-phase unbalanced system is defined as follows:

$$\begin{cases} \overline{V}_1 = \overline{V}_d + \overline{V}_i + \overline{V}_o \\ \overline{V}_2 = a^2 \overline{V}_d + a \overline{V}_i + \overline{V}_o \\ \overline{V}_3 = a \overline{V}_d + a^2 \overline{V}_i + \overline{V}_o \end{cases} \quad \text{with: } a = e^{j\frac{2\pi}{3}}$$

The actual system  $(\overline{V}_1, \overline{V}_2, \overline{V}_3)$  can be deduced from the following three systems:

- direct system  $\overline{V}_d, a^2 \overline{V}_d, a \overline{V}_d$  : three vectors of the same module and phase shifted by  $\frac{2\pi}{3}$  ;

- inverse system  $\bar{V}_i, a\bar{V}_i, a^2\bar{V}_i$ : three vectors of the same module and phase shifted by  $\frac{4\pi}{3}$ ;
- homopolar system  $\bar{V}_0, \bar{V}_0, \bar{V}_0$ : which is zero because of star-connection adopted.

Vectors  $(\bar{V}_d, \bar{V}_i, \bar{V}_0)$  are defined from  $(\bar{V}_1, \bar{V}_2, \bar{V}_3)$  by using Fortescue transformation as following:

$$\begin{cases} \bar{V}_d = \frac{1}{3}(\bar{V}_1 + a\bar{V}_2 + a^2\bar{V}_3) \\ \bar{V}_i = \frac{1}{3}(\bar{V}_1 + a^2\bar{V}_2 + a\bar{V}_3) \\ \bar{V}_0 = \frac{1}{3}(\bar{V}_1 + \bar{V}_2 + \bar{V}_3) \end{cases} \quad \text{with: } a = e^{j\frac{2\pi}{3}}$$

By applying this transformation, to the obtained two-phase short-circuit system (in steady state), we can express it as follows:

$$\begin{pmatrix} \bar{I}_{d_{2ph}} \\ \bar{I}_{i_{2ph}} \\ \bar{I}_{O_{2ph}} \end{pmatrix} = M_f \cdot \begin{pmatrix} \bar{I}_{1_{2ph}} \\ \bar{I}_{2_{2ph}} \\ \bar{I}_3 = 0 \end{pmatrix} \quad \text{where } M_f = \begin{bmatrix} 1 & a & a^2 \\ 1 & a^2 & a \\ 1 & 1 & 1 \end{bmatrix} \quad \text{and } a = e^{j\frac{2\pi}{3}}. \quad (3)$$

Expression (3) represents the two obtained balanced direct and inverse systems and the homopolar system is zero because of star-connection of the electrical machine.

## PM eddy-current loss calculation during unbalanced short-circuit

The analytical model used to estimate the PM eddy-current losses to resistance-limited (i.e., without eddy-current reaction field) is fully explained in [7-8]. It is based on the model proposed by [9-10], formalized to express the evolution of harmonic PM resistance as function of frequency. This model takes into account both spatial and time harmonics, circumferential segmentation effect of PMs and rotation of the rotor.

In order to calculate this losses during unbalanced short-circuits, we apply this analytical model to direct and inverse current system, assuming that total losses are the sum of the ones created by each system (linear behavior).

The results of the comparison between the analytical model and 2-D finite-element simulations are shown in Figure 5, highlighting a quite good agreement between analytical and numerical calculations. In addition, Figure 5-(b) shows that the two-phase short-circuit leads to more than ten times higher losses than balanced three-phase short-circuit. It is clearly due to the inverse system due to unbalanced currents, which create a high rotating field having the same amplitude than the direct one, but turning in the opposite direction of the rotor.

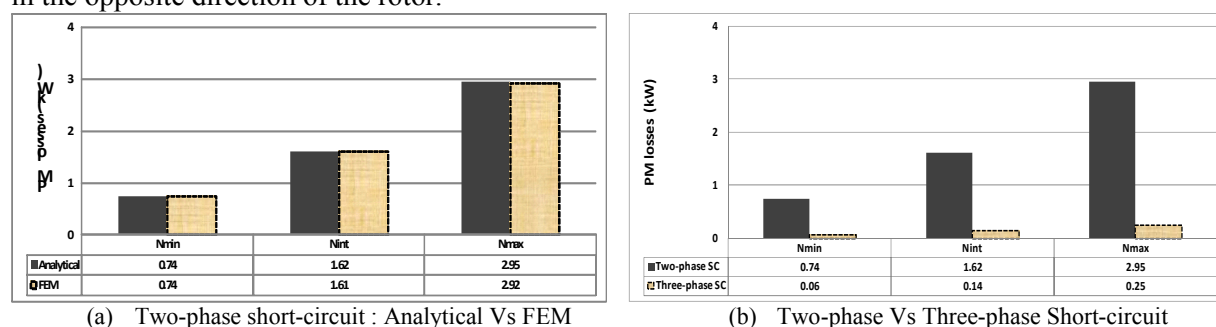


Fig.5 : PM eddy-current losses during short-circuit as function of speed

## Short-circuit electromagnetic torque calculation

Short-circuit electromagnetic torque is created by the interaction of the magnetic field created by the PMs and short-circuit currents. The estimated electromagnetic torque reflecting the mechanical behavior of the machine is key information for system mechanical design. The calculation of electromagnetic torque is based on Maxwell's tensor method. The electromagnetic torque is given by:

$$C_{em}(t) = -R_{sc}^2 \cdot p \cdot L_m \int_0^{2\Theta_p} J(\Theta_s, t) \cdot B_{rad}(R_{sc}, \Theta_s, t) \cdot d\Theta_s \quad (4)$$

where  $\Theta_p$  is the mechanical angle of a pole-pitch,  $J(\Theta_s, t)$  the stator current surface density (at the level of the external surface of the stator, when suppressing the teeth by using Carter coefficient), and  $B_{rad}(R_{sc}, \Theta_s, t)$  the air-gap flux density created by the PMs where the developed expression is given for example in [6].

After calculation, the electromagnetic torque can be expressed as follows:

$$C_{em}(t) = B_{rac} \cdot S_{cylc} \sum_{g=0}^{N_{ph}-1} \sum_n \left[ \frac{p \cdot R_{sc}}{b_{oec}} \cdot K_m(n) \cdot \left[ C_l(n) + D_l(n) \cdot \left( \frac{R_a}{R_{sc}} \right)^{np+2} \right] \right] \times n \cdot i_{ccg}(g, n, t) \cdot \sin \left( n \cdot p \cdot \Theta_{rs}(t) - n \cdot g \cdot \frac{2\pi}{N_{ph}} \right) \quad (5)$$

where  $N_{ph}$  is the number of phases.

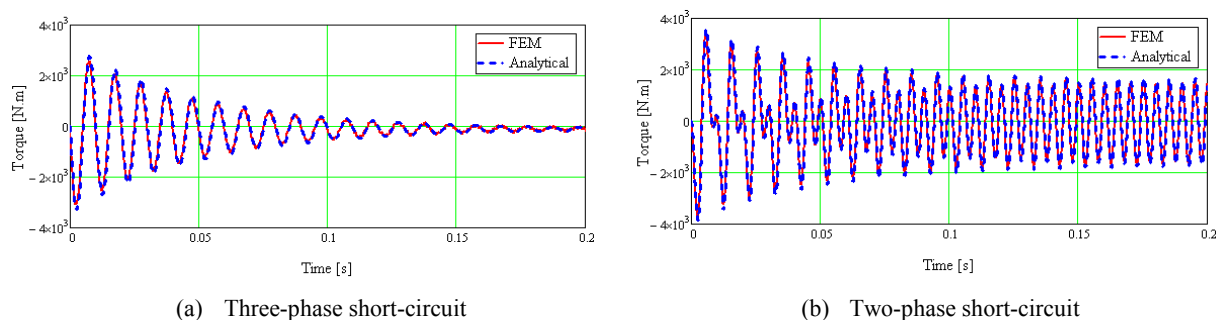


Fig.6. Short-circuit electromagnetic torque

The obtained results are shown in Figure 6, where once again we can notice that analytical modeling agree well with finite-element results. As for PM eddy-current losses, we can notice that unbalanced short-circuit and the corresponding reverse rotating field is the most damaging to the mechanical transmission.

## Experimental results during three-phase short-circuit

Both analytical and numerical models have been validated with experimental results. The experimental test bench presented Figure 7 includes a 7 kW PMSM designed in our laboratory, driven by an induction motor fed by a three phase power inverter. The parameters of the tested PMSM are listed below:

- Rated power: 7 kW
- Rated torque: 100 N.m
- Maximal transient torque (< 30s): 200 N.m
- Rated speed: 668 rpm
- Maximal speed: 4200 rpm

Pole pairs: 6  
 Fundamental flux: 0,3174 Wb  
 Phase resistance: 0,42  $\Omega$   
 Cyclic inductance: 9,28 mH  
 Torque measurement accuracy:  $\pm 2,5$  N.m

The three-phase short-circuit current and the electromagnetic torque have been measured to validate the models presented in this paper. These tests have been done gradually and at low speed to prevent damage against the machine, especially demagnetization of PMs due to simultaneous overheating and high demagnetization field.



Fig.7 : Experimental test bench

The obtained results are given in Figure 8. However, despite the simplicity of the proposed method, the results are satisfactory. Two-phase short-circuit measurements are very difficult to achieve. Indeed, high torque ripples make the speed control very difficult at low speeds, so that it was nearly impossible to obtain a constant speed with our test bench.

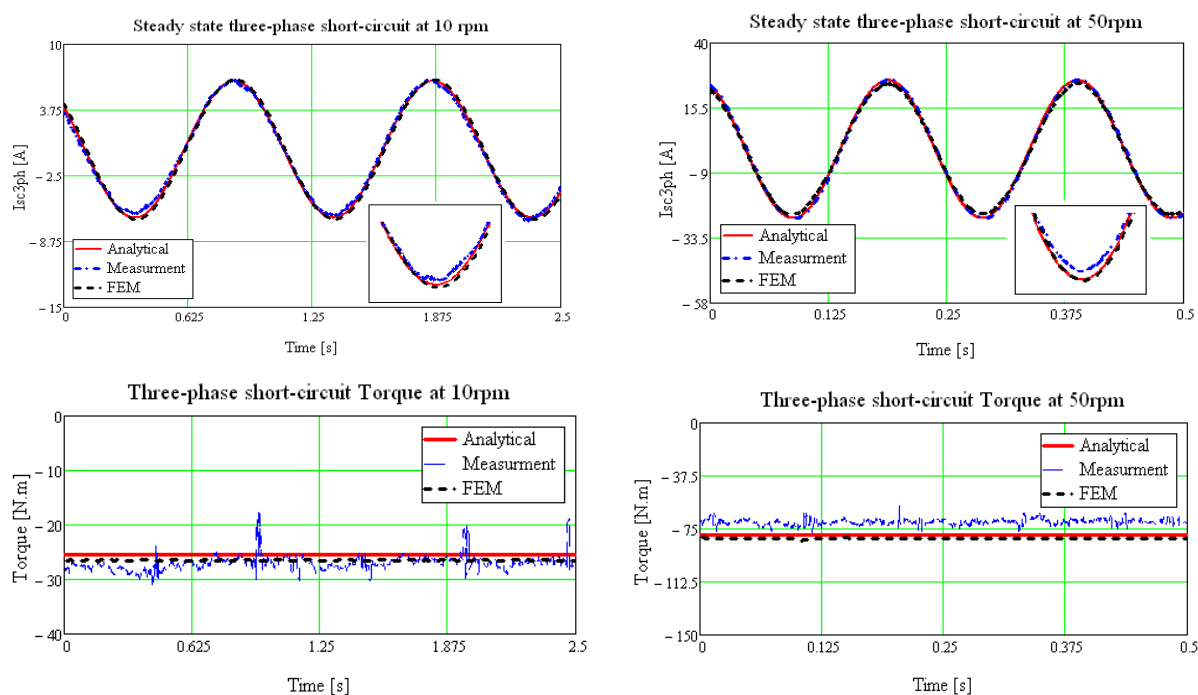


Fig.8 : Three-phase short-circuit Current and Torque (Analytical Vs Measurement Vs FEM)

## Conclusion

In this paper, an accurate analytical modeling of PMSM motors short-circuits has been proposed. The analytical calculation of steady state PM eddy-current losses to resistance-limited agrees pretty well with finite-element modeling. Short-circuit currents and electromagnetic torque has been validated at steady state by using results of finite-element simulations and tests.

The analytical results show that the two-phase short-circuit is the most harmful for the machine because of coexistence of direct and inverse rotating magnetic fields (with comparable magnitudes) which were introduced using Fortescue's transformation.

The consequences of defaults such as short-circuits must be integrated in the design process and optimization of electrical machines, in order to find solutions to weaken them, or at least to prevent motor deteriorations in degraded mode. This can be achieved efficiently with the model proposed in this paper: the calculation of torques enables the mechanical design, and the calculation of PM losses enables to design the motor cooling system (considering fault operation) and also enables to prevent the PM demagnetization. These considerations are all the most important for traction applications, because the availability of the drive is directly linked to availability of the train and thus the schedule adherence.

## References

- [1] C. L. Fortescue, "Method of Symmetrical Co-Ordinates Applied to the Solution of Polyphase Networks," in American Institute of Electrical Engineers, July 1918.
- [2] B. A. Welchko, T. M. Jahns, W. L. Soong, and J. M. Nagashima, "IPM synchronous machine drive response to symmetrical and asymmetrical short circuit faults," in Proc. 9th Eur. Power Electron. Applicat., 2001.
- [3] B. A. Welchko, T. M. Jahns, W. L. Soong, and J. M. Nagashima, "IPM synchronous machine drive response to symmetrical and asymmetrical short circuit faults," in Proc. 9th Eur. Power Electron. Applicat., 2001.
- [4] W. Soong and T. J. E. Miller, "Field-Weakening performance of brushless synchronous AC motor drives," Proc. Inst. Elect. Eng.- Electr. Power Applicat., vol. 141, no. 6, pp. 331–339, 1994.
- [5] T.F. Chan, W. Wang and L.L. Lai, "Permanent-Magnet Synchronous Generator Supplying an Insulated Load", IET Electrical Power Applications Vol.4, No.3, pp 169-176, 2010.
- [6] F. Dubas and C. Espanet, "Slotting Effect in Permanent-Magnet Motors via a 2-D Exact Sub-Domain Model", in Proc. ELECTRIMACS, Cergy-Pontoise (France), June 2011.
- [7] M. Sough, D. Depernet, F. Dubas, B. Boualem, C. Espanet, "Analytical Modeling of Permanent Magnet Losses -Harmonic Equivalent Resistance of PM", in International Conference on Electrical Machine and Systems ICEMS, Sep 2011.
- [8] M. Sough, D. Depernet, F. Dubas, B. Boualem, C. Espanet, "Analytical Model of PMSM Designed for High-Frequency Operation – Machine and Inverter Sizing Compromise", in Energy Conversion Congress & Exposition ECCE, Sep 2011.
- [9] K. Atallah, D. Howe, P.H. Mellor, and D.A. Stone, "Rotor loss in permanent magnet brushless AC machines", IEEE Trans. Ind. Appl., vol.36, no. 6, pp. 1612–1618, Nov.–Dec. 2000.
- [10] D. Ishak; Z.Q. Zhu, and D. Howe, "Eddy-Current Loss in the Rotor Magnets of Permanent-Magnet Brushless Machines Having a Fractional Number of Slots Per Pole", IEEE Trans. Magn., vol. 41, no.9, pp. 3728–3726, Sep. 2005.